Astronomy & Astrophysics manuscript no. output
October 16, 2022

Dating young open clusters using δ Scuti stars

Results for Trumpler 10 and Praesepe

D. Pamos Ortega, A. García Hernández, and J.C. Suárez Yanes

Departamento de Física Teórica y del Cosmos, Universidad de Granada, Campus de Fuentenueva s/n, 18071, Granada, Spain
e-mail: davidpamos@correo.ugr.es

ABSTRACT

Aims. The main goal of this work is to advance towards a reliable way to help date young open clusters, using δ Sct stars. Seismic indices as the large separation, the frequency at maximum power and the splitting of frequencies of the same order and degree, can help to constrain the models in order to characterize the stars as best as possible. We have added a reliable method to identify some radial modes, in order to reduce the uncertainty in determining the age of a δ Scuti star group, belonging to the same young open cluster.
Methods. The method consists of the following steps: 1) Constrain the models of a grid built with the typical parameters of δ Sct stars, via these seismic indices. 2) Compare the frequency ratios between the observed frequencies and the models, in order to select those frequencies with ratios that are within the range of the ratios between the fundamental mode and the radial overtones predicted by the models. 3) Once we have set a range of possible values for some radial modes at the observed frequencies, mainly the fundamental mode, cross check with the models to determine an age range for each analysed star. 4) Assuming this star group have similar chemistry and age, extract the range of common ages to determine the possible age of the entire group.
Results. Using this method, we have estimated the common ages of two δ Scuti groups belonging to two different open clusters: one in Trumpler 10, between 15 and 79 Myr, and another in Praesepe, between 850 and 952 Myr.

Key words. asteroseismology – delta Scuti stars – open clusters

1. Introduction

Determining the age of a star is essential to know its internal physics. Regarding dating a star cluster, the importance lies in understanding the structure and evolution of the galaxy. However, the age is not a direct observable, and then to infer it with enough accuracy is not an easy task. In addition, the ambiguity is greater since we cannot be sure that all the stars in the cluster formed at the same epoch. Especially if it is a globular cluster, where the age is great enough so that different populations, or generations, of stars may coexist within it (Bastian & Lardo 2018). For example, Costa et al. (2019) found two distinct populations of 176 Myr and 288 Myr stars in NGC 1866, combining an analysis of its best-studied Cepheids, with that of a very accurate colour-magnitude diagram (CMD) obtained from the Hubble Space Telescope photometry. Nonetheless, the confidence with which we can date a young open cluster using a small sample of well-characterized stars is greater, assuming that there is likely one star formation epoch (Krause et al. 2020).

Traditionally, isochrone fitting on the HR diagram has been used to date a star cluster. This method is reliable enough when dealing with an old globular cluster, where we can find a large sample of stars leaving the main sequence, and evolving towards the turn-off branch. However, the ambiguity of this method is greater with young clusters, with a majority of stars still on the main sequence. The method based on spectroscopic observations of lithium (Basri & Martín 1999; Stauffer et al. 1999) also generates great ambiguities due to unresolved binary stars (Martín et al. 2001), or its great dependence on representative models that take into account the physics of the stellar atmosphere. The relation between rotation and age of late F to M stars, called gyrochronology (Barnes 2003), seems to provide a method with which to reduce the uncertainty in determining the age of evolved clusters. Also the methods based on chemical clocks (da Silva et al. 2012; Spina et al. 2017; Moya et al. 2022) seem to help in the same direction, making use of machine learning techniques. The drawback is that these algorithms are trained with models of highly evolved stars, in which it has been possible to obtain reliable spectroscopic observations. Therefore, despite the progress achieved with these new techniques, we still do not have a reliable method for dating young open clusters.

In Pamos Ortega et al. (2022) (DPO22 from now on), we proposed the use of seismic parameters for dating a δ Scuti star group belonging to the young open cluster α *Per*, with a resulting common age between 96 and 100 Myr. One of these seismic indices is the large separation, defined as the difference between acoustic modes of the same degree and consecutive orders, related to the mean density and the surface gravity of the star. This regularity in the frequency pattern has been also found in the low order regime (n = [2, 8]) (Suárez et al. 2014; García Hernández et al. 2015, 2017). Another one is the frequency at maximum power, directly related to the effective temperature, used in solar-type stars, found in δ Sct stars as well (Barceló Forteza et al. 2018, 2020; Bowman & Kurtz 2018; Hasanzadeh et al. 2021). In this work, we continue to take steps towards an accurate way to date young open clusters, by including key information from radial modes. To do so, we developed a new method to reliably identify them.

The structure of the paper is as follows: in Sec. 2 we provide the estimated ages of the clusters Trumpler 10 and Praesepe in

previous works. In Sec. 3 we expose the sample of δ Sct stars used in this research. In Sec. 4 we show their seismic parameters. In Sec. 5 we describe the details of the grid of models built for characterizing our δ Sct stars. In Sec. 6 we explain the method for estimating a range for the fundamental mode and the radial overtones. In Sec. 7 we discuss the reliability of our results by comparing them with the observed parameters. And finally, in Sec. 8, we expose the main conclusions of our research and the next steps to improve the method.

2. The ages of Trumpler 10 and Praesepe

Trumpler 10 (C 0846-423) is an open cluster located in the constellation Vela. According to the Milky Way Star Clusters (MWSC) catalog (Kharchenko et al. 2013), it is at a distance of about 417 pc from the Sun and has an age of about 24 Myr. In this survey, stellar parameters as age were computed using the Padova isochrones with solar metallicity (Z = 0.019), with an error of about 25%.

On the other hand, Praesepe (M44, NGC2632) is an open cluster located in the constellation Cancer. Also taking as reference the MWSC survey, it is at a distance of about 187 pc and has an age of about 729 Myr, with an error of about 10%. The value of Z = 0.094 for this cluster in the MWSC was taken from the literature. Being one of the closest clusters to the sun, it is also one of the most studied (see for example Suárez et al. 2002; Brandt & Huang 2015; Choi et al. 2016; Cummings et al. 2017; Gaia Collaboration et al. 2018, and references therein). Recently, Douglas et al. (2019) estimated an age of 670 ± 67 Myr. Actually, they calculated the age of the open cluster Hyades, using a gyrochronology model tuned with slow rotators in Praesepe and the Sun, assuming that both clusters are coeval, based on the similarity of their CMDs, activity, rotation and lithium abundance.

3. The data

Firstly, we have done a cross match between the VizieR Online Data Catalogue Gaia DR2 of open cluster members (Cantat-Gaudin et al. 2018) and the TESS Input Catalogue (TIC) (Stassun 2019), searching possible δ Sct stars belonging to the same open cluster.

According to the definition of a pure δ Scuti from Grigahcène et al. (2010) and Uytterhoeven et al. (2011), we have found a list of 5 good candidates in the field of Trumpler 10 (see Fig. 1 and Tab. 1) and a list of 6 good candidates in the field of Praesepe (see Fig. 2 and Tab. 2).

Regarding Trumpler 10, we have analyzed our sample using data from sector 35 of the *TESS* mission (Ricker et al. 2014), with approximately 13800 points; and from sector 45 for Praesepe, with approximately 15500 points. In both cases, the Rayleigh resolution is approximately 0.041 d^{-1} and the cadence, around two minutes. We have used the Pre-Search Data Conditioned (PDC) light curves, corrected for instrumental effects, that are publicly available through the TESS Asteroseismic Science Consortium (TASC)[1].

Using MultiModes[2], we have extracted the frequency content of each star in our sample. It is a python code that calculates the Fast LombScargle (Press & Rybicki 1989) of a light curve. It extracts, one by one, a limited number of significant signals, and uses their corresponding parameters (amplitudes, frequencies) to fit the total signal to a multisine function with a non-linear least squares minimization. We have adopted as stop-criterion the signal to noise relation SNR > 4.0 (Breger et al. 1993), and we have filtered possible frequency combinations. The code is explained in detail in DPO22 and in the public repository.

Fig. 3 and Fig. 4 show, respectively, the extracted frequency spectrum of each δ Scuti candidate in Trumpler 10 and Praesepe. The values of the first ten extracted frequencies for each star in both clusters are shown in Tab. 3. The whole table with all the extracted frequencies are only available on-line.

4. Seismic parameters

Sometimes it is possible to find regularities in the complex frequency pattern of a δ Scuti star (García Hernández et al. 2009; Paparó et al. 2016; Bedding et al. 2020). Following the same techniques than in García Hernández et al. (2009, 2013); Ramón-Ballesta et al. (2021) and used in DPO22, we have estimated the large separation in the low order regime, $\Delta\nu_{low}$. Fig. 5 is an example of this, where we have used the Discret Fourier Transform (DFT) and the Autocorrelation Diagram (AC) applied on the power spectrum, the Frequency Difference Histogram (FDH) and the Èchelle Diagram (ED), in order to find regularities in the frequency content of TIC 28943819 (see Ap. A for the rest of our sample). Some theoretical works as García Hernández et al. (2009); Reese et al. (2017) use the AC and the FT to search for the low-order large separation and the rotational splitting. They pointed out that its half value is visible in the FT, as it is this case.

We have also estimated the frequency at maximum power, following the method in Barceló Forteza et al. (2020), in order to use a relation between $\nu_{\max}$ and the effective temperature obtained with a sample of pure δ Sct stars. We have taken $\nu_{\max}$ as the average frequency weighted over the amplitudes:

$$\nu_{max} = \frac{\sum A_i \cdot \nu_i}{\sum A_i} \tag{1}$$

The seismic temperature, $\tilde{T}_{\rm eff}$, is calculated with Eq. 2, with a dispersion value of $\sigma = 3.36\%$:

$$\tilde{T}_{\rm eff} = (3.5 \pm 0.1)\nu_{max}(\mu Hz) + (6460 \pm 40)\ (K) \tag{2}$$

The estimated values for $\Delta\nu_{low}$, $\nu_{\max}$ and the corresponding seismic temperatures $\tilde{T}_{\rm eff}$ for our sample of δ Sct stars in Trumpler 10 and Praesepe are shown in Tab. 4 and Tab. 5, respectively.

It has not been possible to see rotational splitting with any of the stars analyzed from Trumpler 10 and Praesepe. Then we cannot deduce a rotational frequency from this seismic parameter. This was indeed possible with two stars from the α Per cluster in DPO22.

5. The grid of models

In the case of δ Sct stars, which rotate between moderate and fast, the models have to take into account the stellar structure deformation that occurs at these speeds. This determines the value of the internal parameters, such as the density, directly related to one of the seismic indices that we are using here, the large separation. For this reason, we have calculated our models with the MESA (Paxton 2019) and FILOU (Suárez & Goupil 2008) codes, taking rotation into account up to second order in the pertubative theory for the adiabatic oscillation computation (including

[1] https://tasoc.dk
[2] https://github.com/davidpamos/MultiModes

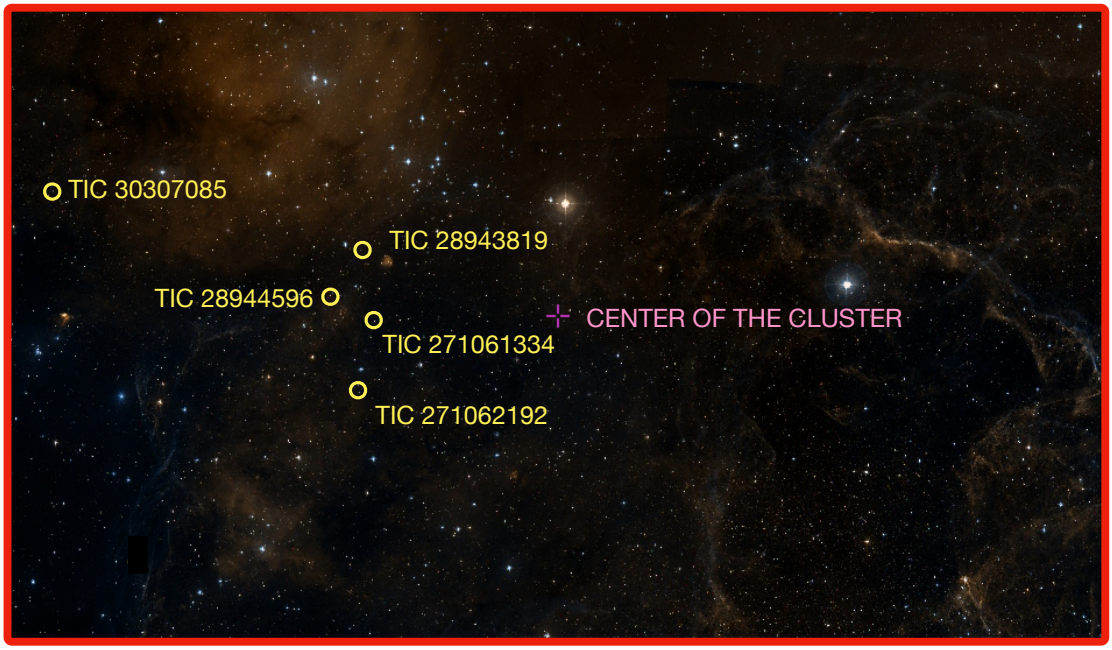

Fig. 1: The five selected targets in the field of Trumpler 10

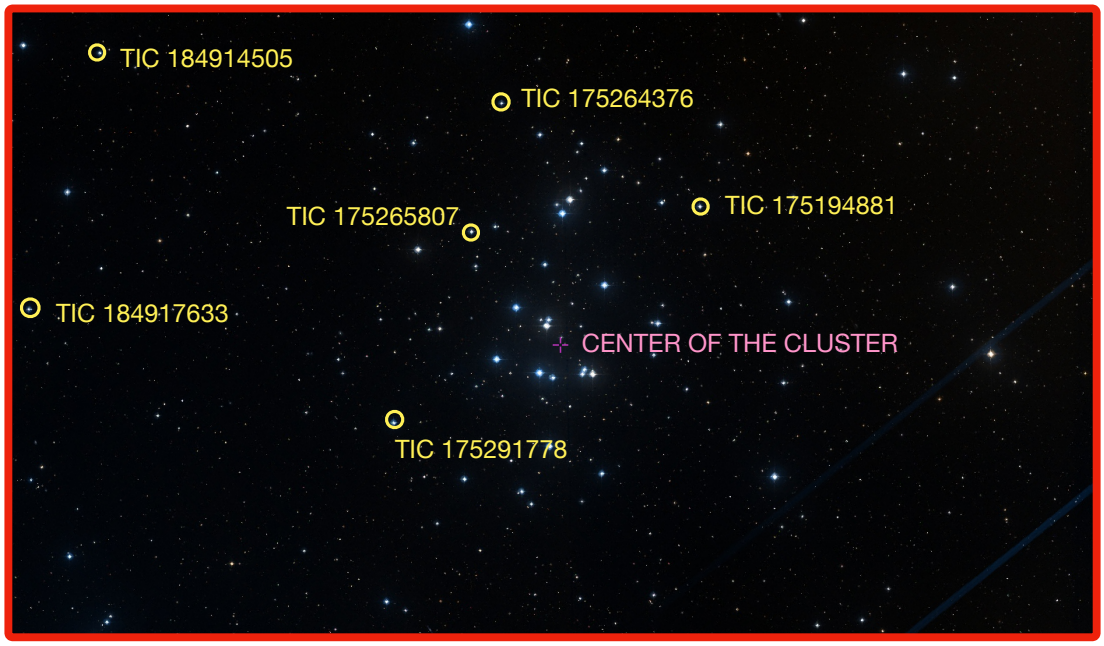

Fig. 2: The six selected targets in the field of Praesepe

Table 1: Stellar parameters of the selected targets in Trumpler 10. References: [1]Stassun (2019), [2]Cantat-Gaudin et al. (2018)

TIC	$M(M_\odot)^1$	$R(R_\odot)^1$	$\bar{\rho}(\bar{\rho}_\odot)$	$logg^1$	$T_{\rm eff}(K)^1$	P^2_{member}
28943819	2.2 ± 0.3	1.60 ± 0.06	0.53 ± 0.14	4.37 ± 0.08	8646 ± 161	1.0
30307085	2.5 ± 0.3	1.47 ± 0.04	0.80 ± 0.17	4.51 ± 0.06	9931 ± 202	0.8
28944596	2.1 ± 0.3	1.72 ± 0.06	0.41 ± 0.10	4.28 ± 0.07	8383 ± 149	1.0
271061334	2.2 ± 0.3	1.58 ± 0.05	0.56 ± 0.13	4.38 ± 0.07	8773 ± 170	0.9
271062192	2.2 ± 0.3	1.68 ± 0.05	0.46 ± 0.11	4.33 ± 0.07	8689 ± 158	1.0

Table 2: Stellar parameters of the selected targets in Praesepe. References: [1]Stassun (2019), [2]Cantat-Gaudin et al. (2018)

TIC	$M(M_\odot)^1$	$R(R_\odot)^1$	$\bar{\rho}(\bar{\rho}_\odot)$	$logg^1$	$T_{\rm eff}(K)^1$	P^2_{member}
175194881	1.9 ± 0.3	2.10 ± 0.07	0.20 ± 0.05	4.07 ± 0.08	7873 ± 125	1.0
175264376	1.7 ± 0.3	2.13 ± 0.09	0.17 ± 0.05	4.01 ± 0.08	7416 ± 141	1.0
175265807	1.9 ± 0.3	1.92 ± 0.06	0.26 ± 0.07	4.14 ± 0.08	7826 ± 126	1.0
175291778	1.9 ± 0.3	2.31 ± 0.06	0.15 ± 0.04	3.98 ± 0.08	7865 ± 126	1.0
184914505	1.7 ± 0.3	1.94 ± 0.06	0.23 ± 0.06	4.09 ± 0.08	7369 ± 108	1.0
184917633	1.7 ± 0.3	2.08 ± 0.07	0.19 ± 0.05	4.03 ± 0.08	7443 ± 122	1.0

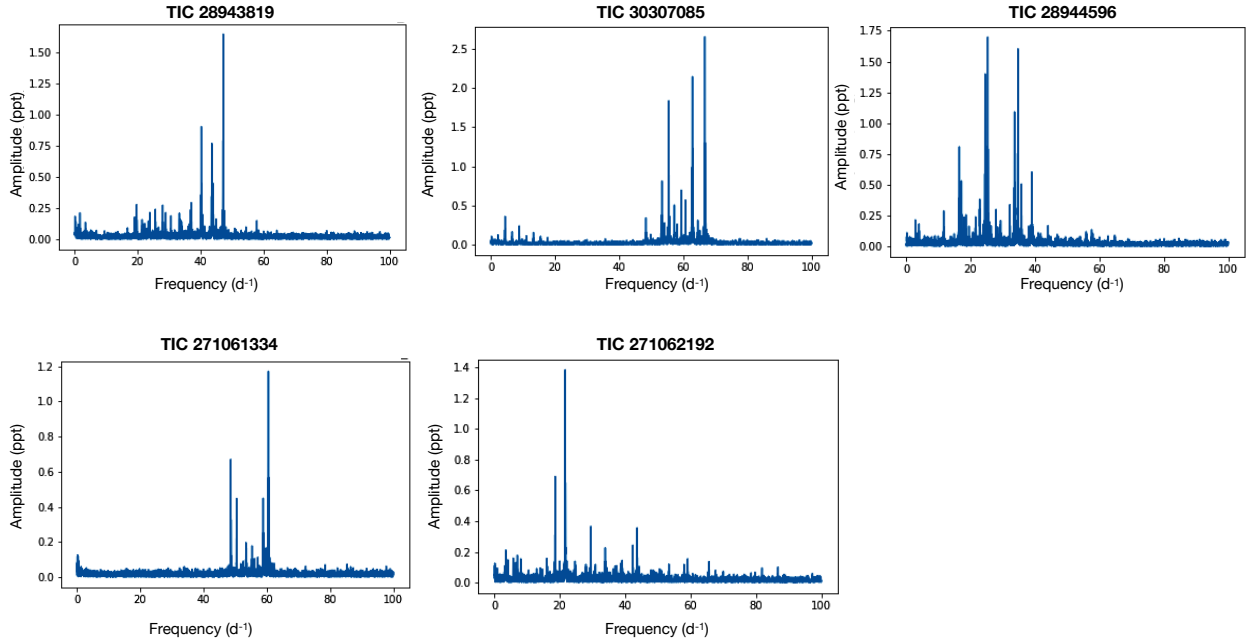

Fig. 3: Frequency spectrum of the sample of δ Sct stars candidates in the field of Trumpler 10

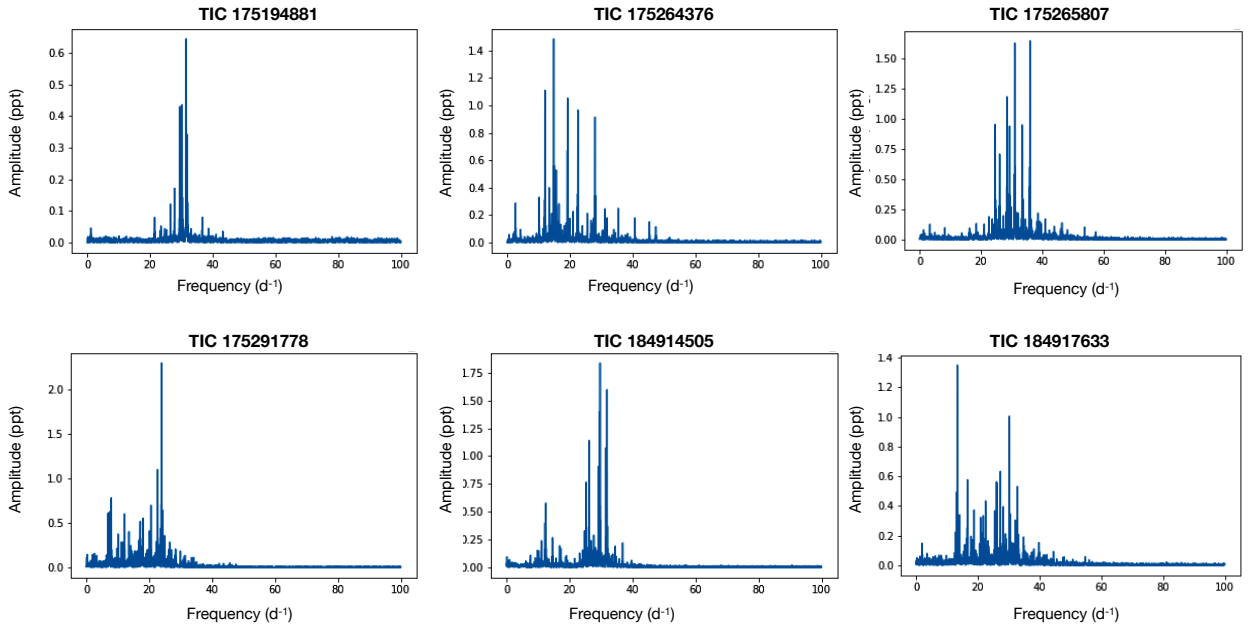

Fig. 4: Frequency spectrum of the sample of δ Sct stars candidates in the field of Praesepe

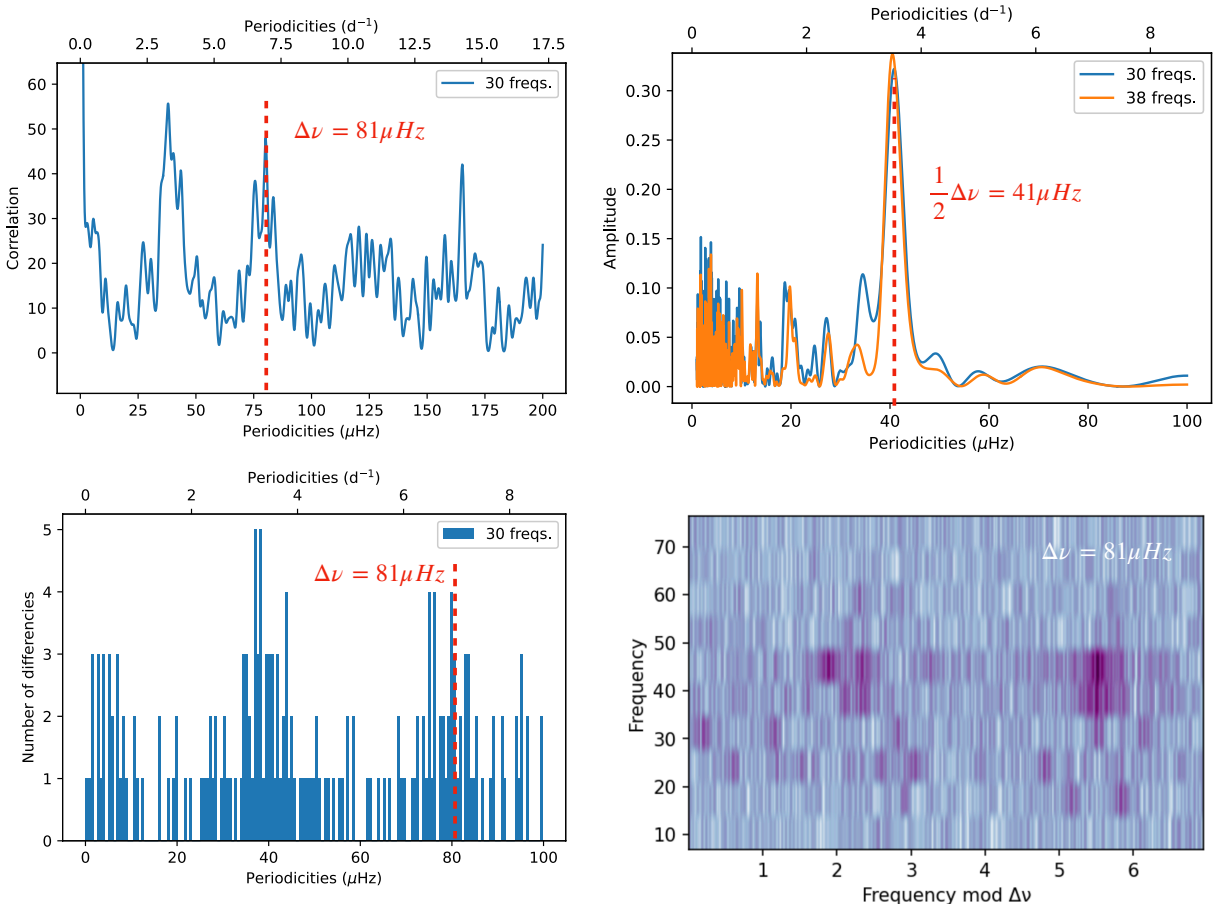

Fig. 5: Estimated large separation for TIC 28943819, using the Autocorrelation Diagram (top left), the Discrete Fourier Transform (top right), the Frequency Difference Histogram (bottom left), and the Èchelle Diagram (Hey & Ball 2020) (bottom right)

near-degeneracy effects and stellar structure deformation). Following the same line of DPO22, we have built a grid of models to characterize δ Sct stars during their stay on the main sequence, from *Zero Age Main Sequence* (ZAMS) to *Terminal Age Main Sequence* (TAMS). In this new grid we have incorporated, as a free parameter, the core overshooting (see Fig. 6). In the ZAMS it does not have a large value, but it can be high enough near the TAMS, so that it can significantly lengthen the stay of the star in the main sequence. As it can be seen in Tab. 6, we have taken the null value as the lower limit, and the value 0.02 as the upper limit for the exponential free parameter f_{ov}, following the prescriptions of Claret & Torres (2019). The maximum values for the rotation speed are between $0.1\Omega_c$ (the critical angular velocity) and $0.4\Omega_c$, avoiding higher values that may move away from the limits of the perturbative theory. Regarding the frequencies, we have calculated p and g modes of orders between n=1 and n=8, and degrees between l=0 and l=3.

6. The radial overtones identification

According to Breger et al. (2009), the frequency content of δ Sct stars are not in a random distribution. The non-radial frequencies, the vast majority, seem to be grouped around the radial ones. Then, with some δ Sct stars it is possible to delimit a narrow range of frequencies for each radial overtone. The method consists of the following steps:

- Constrain the models using the estimated values of $\Delta\nu_{\rm low}$ and $\tilde{T}_{\rm eff}$ of the star.
- Compare the ratios of the observed frequencies with the models, in order to select those frequencies whose ratios have values within the range of the ratios between the fundamental mode and the radial overtones (n = [2,8]) predicted by the models (see Tab. 7). By this way, we have better age constrained models.
- By applying the method with other stars of the same group, we can estimate a range of common ages for them.

Applying this procedure to our sample, we have been able to further constrain the models. If we use all the possible identified radial modes, we don't have a common age range for each star group in both clusters, because the number of constrained models for each star is too small. Then, in order to obtain a reliable common age range for the entire group in each cluster, we finally have constrained the models by the low-order large separation, the frequency at maximum power and the fundamental mode of each member of the group. Regarding Praesepe, in Fig. 7 we have plot the relations between the large separation and the frequencies corresponding to the radial modes n = [1,8] of all the calculated models. Using a colour bar we have encoded the age constrained models for each star of the Praesepe group, after having performed our mode identification. The Fig. 8 shows the positions and the ranges of the identified radial overtones in the frequency spectrum of these stars. We have not obtained similar positive results with Trumpler 10 (see Fig. 9, where the num-

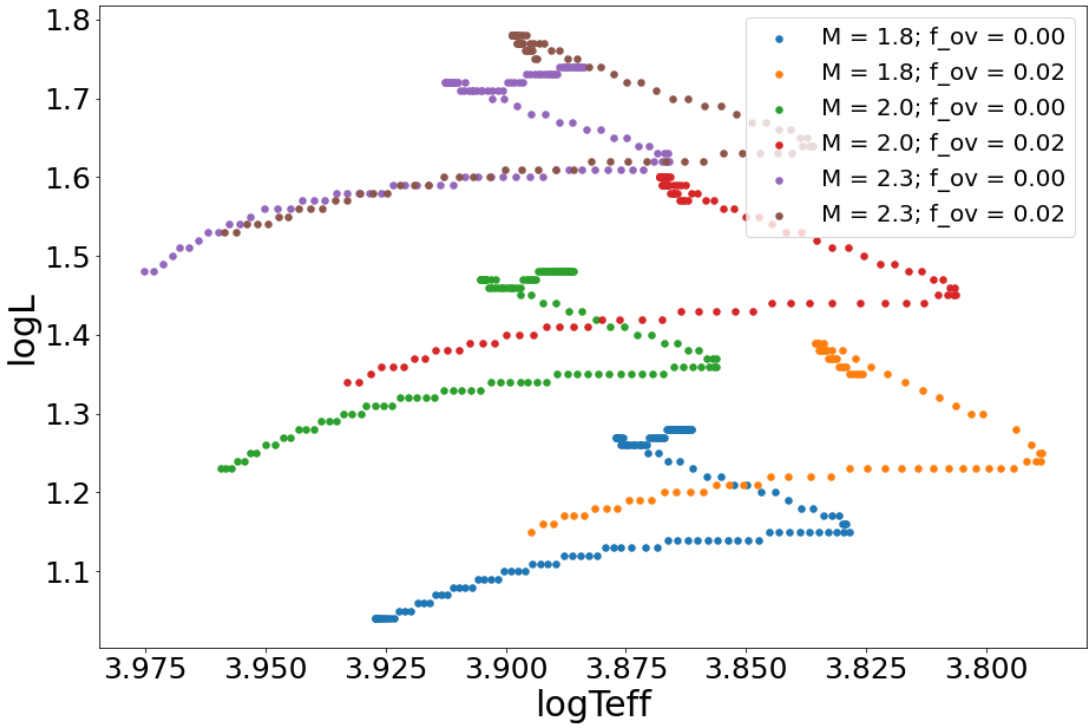

Fig. 6: The overshooting effect in the grid of models calculated with the MESAcode

ber of extracted frequencies in each star has been noticeably less than in the case of Praesepe. Let's remember that Trumpler 10 is further away than Praesepe. This makes it difficult to find observed values that are within the theoretical frequency range (see Fig. 10).

7. Results and discussion

As we can see in the parameters of the constrained models in Tab. 8, the common ages of the star group in Trumpler 10 are between 15 and 79 Myr, assuming they have the same chemistry and age. The similar values of their corresponding observables point to this. We can see that the values of mass, radius and effective temperature are below those of the observed parameters in Tab. 1. The TIC effective temperature is calculated via an empirical color relation, involving the Gaia magnitude, G, and applying an estimated reddening correction. There are many sources of ambiguity when computing a relation between the color magnitude and the effective temperature. Besides, the reddening correction has the effect of making apparently cool stars hotter, and a higher T_{eff} implies a larger radius and mass. Then, these discrepancies between the observed values and the constrained parameters for our sample of stars, may be due to a overestimated reddening in the TIC effective temperature, or due to the effects of gravity darkening caused by the rotation of the star.

The range of common ages for the group of δ Sct stars in Praesepe is between 850 and 952 Myr. Tab. 9 shows the parameters of the models of the Praesepe star group. The models are also in tune with the observed values in Tab. 2, considering that it is a nearby cluster. But also here we can corroborate that the observed values of mass, radius and effective temperature are somewhat higher than those of the constrained models, in particular, in stars where the effective temperature has been obtained by reddening correction: TIC 175194881, TIC 175265807 and TIC 175291778. However, with stars where the effective temperature is spectroscopic: TIC 175264376, TIC 184914505 and TIC 184917633, the agreement is greater. This result points to an age for the cluster somewhat older than previous studies, mentioned in Sec. 2. We cannot rule out the possibility of having found a group of stars of a different generation, belonging to the same cluster, considering that Praesepe is not so young.

8. Conclusions

The use of asteroseismology to characterize the internal physics of δ Sct stars and, by extension, to help date young open clusters, provides promising results. We have tested a seismic method with three open clusters of different ages. With α Per we had obtained the first results in DPO22. In this work we have extended the research to Trumpler 10 and Praesepe and we have applied a method for identifying radial overtones. Regarding Trumpler 10, we have found five δ Sct stars candidates never before classified as such, with common ages between 15 and 79 Myr. Regarding the Praesepe cluster, we have found a new possible δ Scuti star, TIC 184917633. The other five stars from the sample are well known δ Sct stars. We have estimated the age of this star group between 850 and 952 Myr. As we can see in Tab. 8 and Tab. 9, the models are not well constrained in the rotation velocity. It would have been helpful to estimate the rotation frequency with some stars of the group in order to further constrain the models, considering the dependence of the frequency ratios with rotation (Suárez et al. 2006). Then, to advance this strategy, we need a method to help us confidently interpret the rotation frequency in the dense frequency spectrum of δ Sct stars. We also hope that future missions, such as the ESA project HAYDN

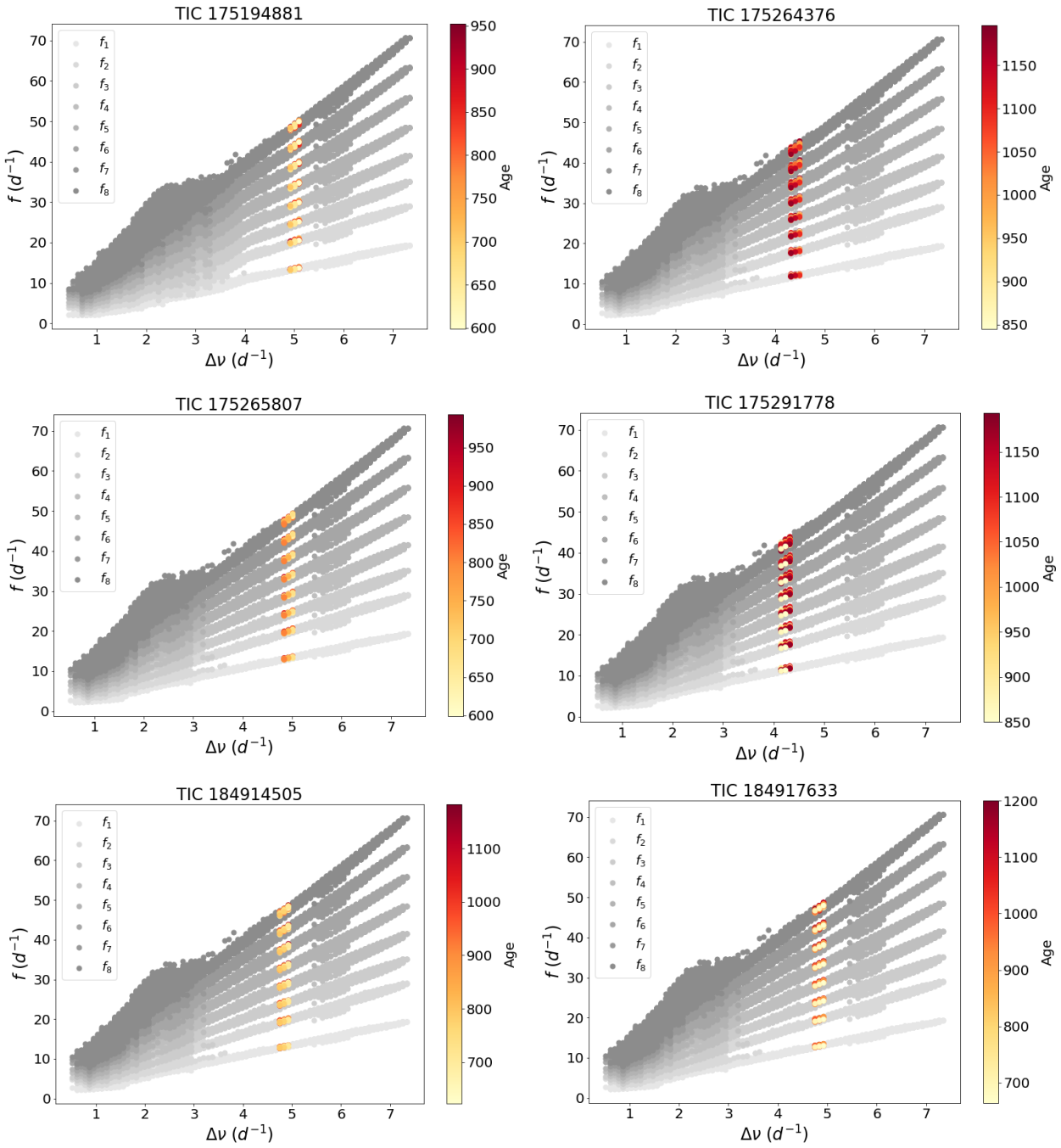

Fig. 7: Relations between the large separation and the radial modes n = [1,8] for our grid of models. Using a colour bar we have encoded the age constrained models for each star of the sample of Praesepe, after having performed our mode identification

("High-precision AsteroseismologY in DenSe stellar fields")[3], will provide high-cadence photometry of stars belonging to clusters, helping to accurately date them.

Acknowledgements. DPO and AGH acknowledge funding support from 'FEDER/junta de Andalucía-Consejería de Economía y Conocimiento' under project E-FQM-041-UGR18 by Universidad de Granada. JCS acknowledges funding support from the Spanish State Research Agency (AEI) project PID2019-107061GB-064.

[3] http://www.asterochronometry.eu/haydn/

References

Barceló Forteza, S., Moya, A., Barrado, D., et al. 2020, A&A, 638, A59
Barceló Forteza, S., Roca Cortés, T., & García, R. A. 2018, A&A, 614, A46
Barnes, S. A. 2003, ApJ, 586, 464
Basri, G. & Martín, E. L. 1999, ApJ, 510, 266
Bastian, N. & Lardo, C. 2018, ARA&A, 56, 83
Bedding, T. R., Murphy, S. J., Hey, D. R., et al. 2020, Nature, 581, 147
Bowman, D. M. & Kurtz, D. W. 2018, MNRAS, 476, 3169
Brandt, T. D. & Huang, C. X. 2015, ApJ, 807, 24
Breger, M., Lenz, P., & Pamyatnykh, A. A. 2009, MNRAS, 396, 291
Breger, M., Stich, J., Garrido, R., et al. 1993, A&A, 271, 482
Cantat-Gaudin, T., Jordi, C., Vallenari, A., et al. 2018, A&A, 618, A93
Choi, J., Dotter, A., Conroy, C., et al. 2016, ApJ, 823, 102
Claret, A. & Torres, G. 2019, ApJ, 876, 134
Costa, G., Girardi, L., Bressan, A., et al. 2019, A&A, 631, A128

Table 3: First ten extracted frequencies, with their corresponding amplitudes, for each star in our samples in Trumpler 10 and Praesepe

Trumpler 10			Praesepe		
TIC	$f(d^{-1})$	A (ppt)	TIC	$f(d^{-1})$	A (ppt)
TIC 28943819	47.185	1.667	TIC 175194881	31.566	0.645
	40.230	0.885		30.242	0.314
	43.554	0.787		29.507	0.426
	44.008	0.463		31.896	0.351
	40.122	0.342		27.811	0.168
	40.359	0.335		26.556	0.117
	37.046	0.318		36.742	0.079
	19.721	0.282		21.457	0.081
	27.977	0.277		23.489	0.051
	36.830	0.251		38.623	0.047
TIC 30307085	66.752	2.630	TIC 175264376	14.845	1.471
	62.280	2.009		12.021	0.914
	55.489	1.809		19.260	1.055
	53.359	0.810		22.514	0.971
	59.387	0.703		27.996	0.919
	60.692	0.548		19.167	0.610
	57.244	0.448		15.575	0.511
	4.427	0.359		13.359	0.394
	48.369	0.344		10.180	0.339
	64.533	0.292		16.501	0.292
TIC 28944596	25.341	1.674	TIC 175265807	35.980	1.629
	34.691	1.588		31.020	1.618
	24.494	1.358		28.457	1.200
	33.649	1.089		24.659	0.975
	16.494	0.815		29.333	0.949
	39.021	0.682		33.417	0.829
	17.145	0.535		33.544	0.812
	35.790	0.513		26.086	0.708
	22.821	0.398		33.794	0.300
	32.201	0.344		28.901	0.262
TIC 271061334	60.529	1.163	TIC 175291778	23.855	2.336
	48.627	0.684		22.667	1.093
	58.877	0.474		7.908	0.790
	50.485	0.455		20.512	0.702
	53.414	0.201		7.332	0.640
	55.330	0.192		24.209	0.631
	53.583	0.168		6.827	0.612
	59.792	0.147		12.141	0.609
	60.696	0.134		18.050	0.546
	0.212	0.157		17.146	0.519
TIC 271062192	21.680	1.397	TIC 184914505	29.667	1.849
	18.611	0.703		31.899	1.543
	29.522	0.367		29.465	1.138
	43.681	0.351		26.145	1.168
	42.380	0.238		31.565	1.059
	33.928	0.224		29.257	0.869
	3.527	0.209		25.231	0.782
	7.028	0.178		12.482	0.591
	59.146	0.157		12.233	0.417
	5.777	0.154		27.690	0.323
			TIC 184917633	13.309	1.359
				30.241	1.019
				27.305	0.613
				16.610	0.581
				26.031	0.531
				32.840	0.526
				26.241	0.518
				22.494	0.435
				13.192	0.402
				28.240	0.409

Table 4: Seismic indices of the selected targets from Trumpler 10

TIC	$\Delta\nu_{\rm low}(\mu$Hz)	$\nu_{\rm max}(\mu$Hz)	$\tilde{T}_{\rm eff}$ (K)
28943819	81 ± 1	510 ± 30	8250 ± 200
30307085	84 ± 1	710 ± 60	8950 ± 320
28944596	75 ± 1	330 ± 80	7620 ± 350
271061334	80 ± 1	650 ± 50	8740 ± 280
271062192	74 ± 1	290 ± 90	7480 ± 380

Table 5: Seismic indices of the selected targets from Praesepe

TIC	$\Delta\nu_{\rm low}$ (μHz)	$\nu_{\rm max}$ (μHz)	$\tilde{T}_{\rm eff}$ (K)
175194881	58 ± 1	350 ± 30	7690 ± 180
175264376	51 ± 1	210 ± 60	7200 ± 270
175265807	57 ± 1	360 ± 40	7720 ± 220
175291778	49 ± 1	200 ± 70	7160 ± 310
184914505	56 ± 1	320 ± 60	7580 ± 280
184917633	56 ± 1	270 ± 80	7410 ± 350

Table 6: Parameters of the stellar structure model grid built with the MESAcode

Parameter	Range	Step
M ($M_\odot$)	[1.6, 2.5]	0.1 $M_\odot$
Z_0	[0.016, 0.020]	0.002
Ω/Ω_c	[0.1, 0.4]	0.1
α	2.0	Fixed
f_{ov}	[0, 0.02]	0.02

Table 7: The fundamental mode and radial overtone ratios in our MESA/FILOU grid of models

Relationship	Range
f_1/f_2	[0.71, 0.90]
f_1/f_3	[0.57, 0.76]
f_1/f_4	[0.49, 0.65]
f_1/f_5	[0.42, 0.57]
f_1/f_6	[0.36, 0.50]
f_1/f_7	[0.32, 0.44]
f_1/f_8	[0.28, 0.40]

Cummings, J. D., Deliyannis, C. P., Maderak, R. M., & Steinhauer, A. 2017, AJ, 153, 128
da Silva, R., Porto de Mello, G. F., Milone, A. C., et al. 2012, A&A, 542, A84
Douglas, S. T., Curtis, J. L., Agüeros, M. A., et al. 2019, ApJ, 879, 100
Gaia Collaboration, Babusiaux, C., van Leeuwen, F., et al. 2018, A&A, 616, A10
García Hernández, A., Martín-Ruiz, S., Monteiro, M. J. P. F. G., et al. 2015, ApJ, 811, L29
García Hernández, A., Moya, A., Michel, E., et al. 2009, A&A, 506, 79
García Hernández, A., Moya, A., Michel, E., et al. 2013, A&A, 559, A63
García Hernández, A., Suárez, J. C., Moya, A., et al. 2017, MNRAS, 471, L140
Grigahcène, A., Antoci, V., Balona, L., et al. 2010, ApJ, 713, L192
Hasanzadeh, A., Safari, H., & Ghasemi, H. 2021, MNRAS, 505, 1476
Hey, D. & Ball, W. 2020, Echelle: Dynamic echelle diagrams for asteroseismology
Kharchenko, N. V., Piskunov, A. E., Schilbach, E., Röser, S., & Scholz, R. D. 2013, A&A, 558, A53
Krause, M. G. H., Offner, S. S. R., Charbonnel, C., et al. 2020, Space Science Reviews, 216

Table 8: Constrained parameters of the models corresponding to our selected targets in Trumpler 10

TIC	$M(M_\odot)$	$R(R_\odot)$	$\bar{\rho}(\bar{\rho}_\odot)$	$\log g$	$T_{\rm eff}$(K)	$log(L/L_\odot)$	v_{rot}(km s^{-1})	$\Delta\nu_{\rm low}(d^{-1})$	Age (Myr)
28943819	[1.7:1.8]	[1.50:1.55]	[0.48:0.50]	[4.30:4.32]	[8056:8450]	[0.93:1.03]	[46:136]	[80:82]	[13:177]
30307085	[1.8:1.9]	[1.50:1.55]	[0.51:0.53]	[4.33:4.34]	[8630:9075]	[1.05:1.16]	[47:95]	[83:84]	[10:79]
28944596	[1.6:1.7]	[1.53:1.56]	[0.44:0.45]	[4.26:4.28]	[7422:7957]	[0.81:0.94]	[131:179]	[74:76]	[15:268]
271061334	[1.8:1.9]	[1.53:1.61]	[0.46:0.50]	[4.30:4.33]	[8460:9008]	[1.04:1.16]	[46:147]	[79:81]	[10:185]
271062192	[1.6:1.7]	[1.54:1.61]	[0.41:0.44]	[4.25:4.27]	[7276:7860]	[0.79:0.93]	[44:198]	[73:75]	[15:473]

Table 9: Constrained parameters of the models corresponding to our selected targets in Praesepe

TIC	$M(M_\odot)$	$R(R_\odot)$	$\bar{\rho}(\bar{\rho}_\odot)$	$\log g$	$T_{\rm eff}$(K)	$log(L/L_\odot)$	v_{rot}(km s^{-1})	$\Delta\nu_{\rm low}(cd^{-1})$	Age (Myr)
175194881	[1.7:1.8]	[1.83:1.95]	[0.24:0.28]	[4.11:4.15]	[7511:7869]	[0.98:1.11]	[41:169]	[57:59]	[602:952]
175264376	[1.6:1.7]	[1.94:2.06]	[0.19:0.22]	[4.03:4.07]	[6943:7469]	[0.92:1.07]	[39:162]	[50:52]	[845:1576]
175265807	[1.7:1.8]	[1.85:1.96]	[0.24:0.27]	[4.10:4.13]	[7504:7937]	[0.99:1.13]	[41:171]	[56:58]	[599:993]
175291778	[1.6:1.8]	[1.97:2.17]	[0.18:0.21]	[4.01:4.06]	[6854:7463]	[0.92:1.11]	[38:161]	[48:50]	[850:1645]
184914505	[1.6:1.8]	[1.84:1.98]	[0.23:0.26]	[4.08:4.13]	[7304:7855]	[0.95:1.12]	[40:167]	[55:57]	[622:1352]
184917633	[1.6:1.8]	[1.84:1.97]	[0.23:0.26]	[4.08:4.12]	[7079:7753]	[0.90:1.09]	[40:167]	[55:57]	[664:1352]

Martín, E. L., Dahm, S., & Pavlenko, Y. 2001, in Astronomical Society of the Pacific Conference Series, Vol. 245, Astrophysical Ages and Times Scales, ed. T. von Hippel, C. Simpson, & N. Manset, 349
Moya, A., Sarro, L. M., Delgado-Mena, E., et al. 2022, A&A, 660, A15
Pamos Ortega, D., García Hernández, A., Suárez, J. C., et al. 2022, MNRAS, 513, 374
Paparó, M., Benkő, J. M., Hareter, M., & Guzik, J. A. 2016, ApJ, 822, 100
Paxton, B. 2019, Modules for Experiments in Stellar Astrophysics (MESA)
Press, W. H. & Rybicki, G. B. 1989, ApJ, 338, 277
Ramón-Ballesta, A., García Hernández, A., Suárez, J. C., et al. 2021, MNRAS, 505, 6217
Reese, D. R., Lignières, F., Ballot, J., et al. 2017, A&A, 601, A130
Ricker, G. R., Winn, J. N., Vanderspek, R., et al. 2014, in Society of Photo-Optical Instrumentation Engineers (SPIE) Conference Series, Vol. 9143, Proc. SPIE, 914320
Spina, L., Meléndez, J., Karakas, A. I., et al. 2017, Monthly Notices of the Royal Astronomical Society, 474, 2580
Stassun, K. G. 2019, VizieR Online Data Catalog, IV/38
Stauffer, J. R., Barrado y Navascués, D., Bouvier, J., et al. 1999, ApJ, 527, 219
Suárez, J. C., García Hernández, A., Moya, A., et al. 2014, A&A, 563, A7
Suárez, J. C., Garrido, R., & Goupil, M. J. 2006, A&A, 447, 649
Suárez, J. C. & Goupil, M. J. 2008, Ap&SS, 316, 155
Suárez, J. C., Michel, E., Pérez Hernández, F., et al. 2002, A&A, 390, 523
Uytterhoeven, K., Moya, A., Grigahcène, A., et al. 2011, A&A, 534, A125

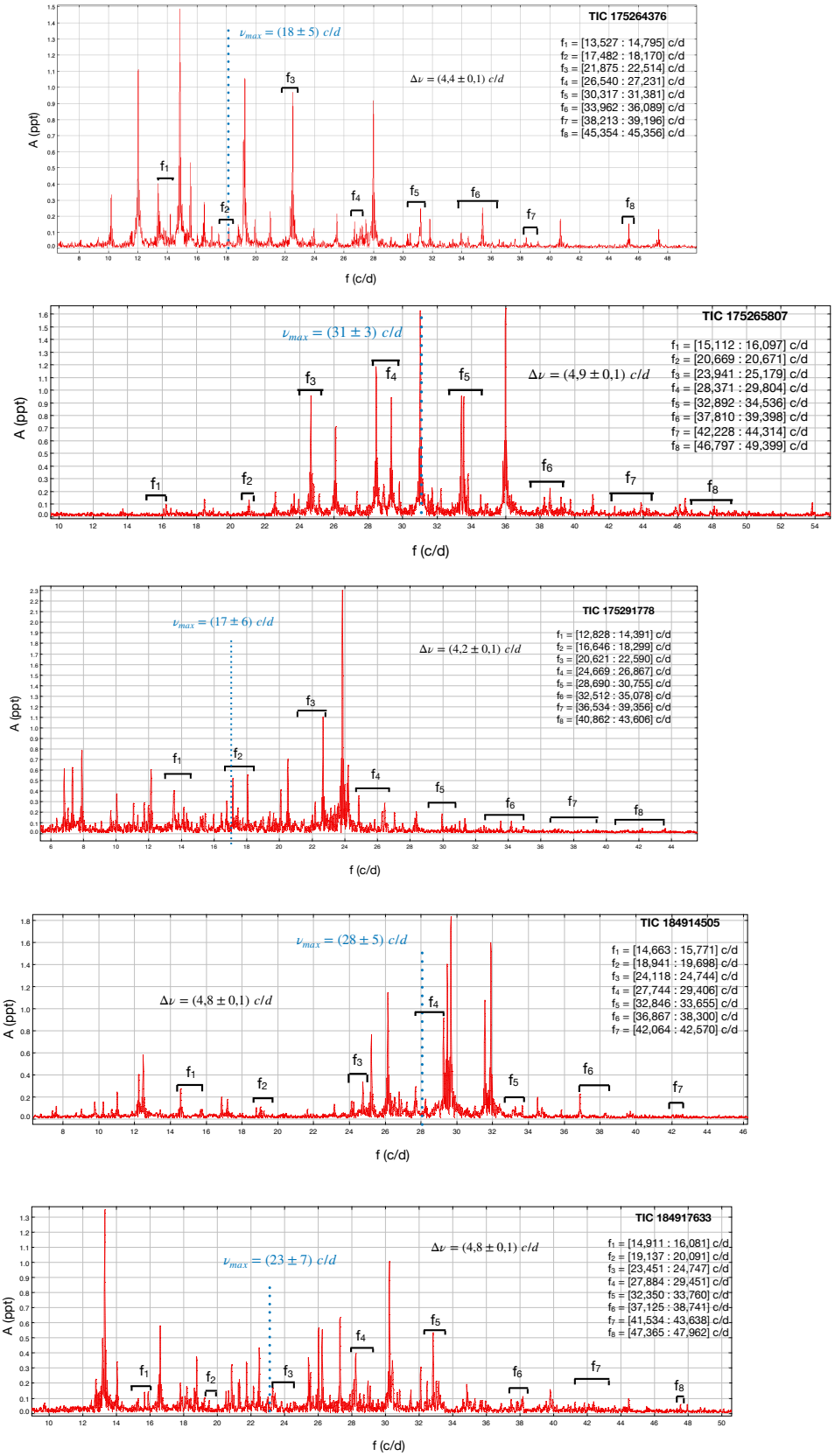

Fig. 8: Identified radial overtones in the frequency spectrum of five of the δ Sct stars candidates in the field of Praesepe

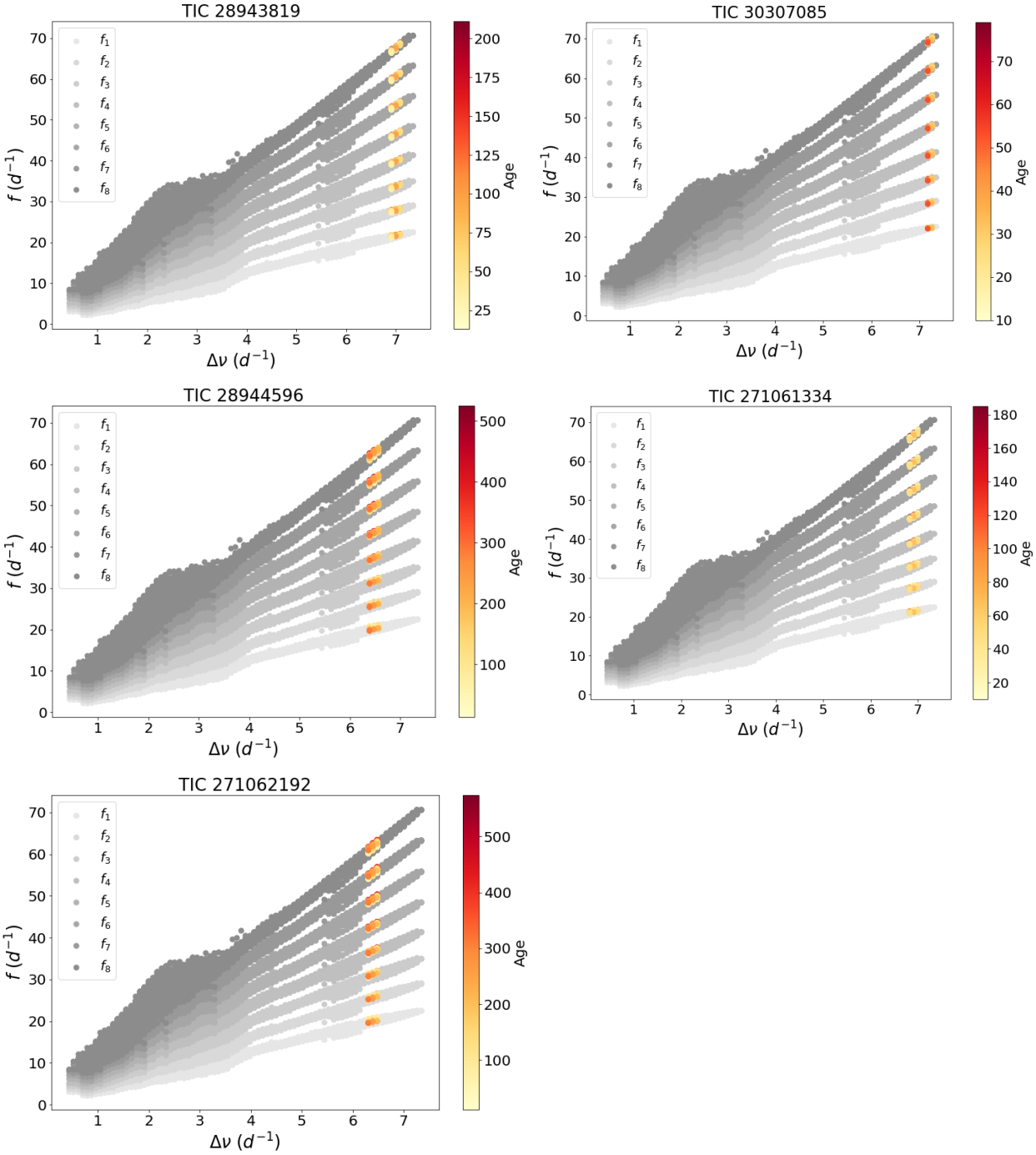

Fig. 9: Relations between the large separation and the radial modes n = [1,8] for our grid of models. Using a colour bar we have encoded the age constrained models for each star of the sample of Trumpler 10, after having performed our mode identification

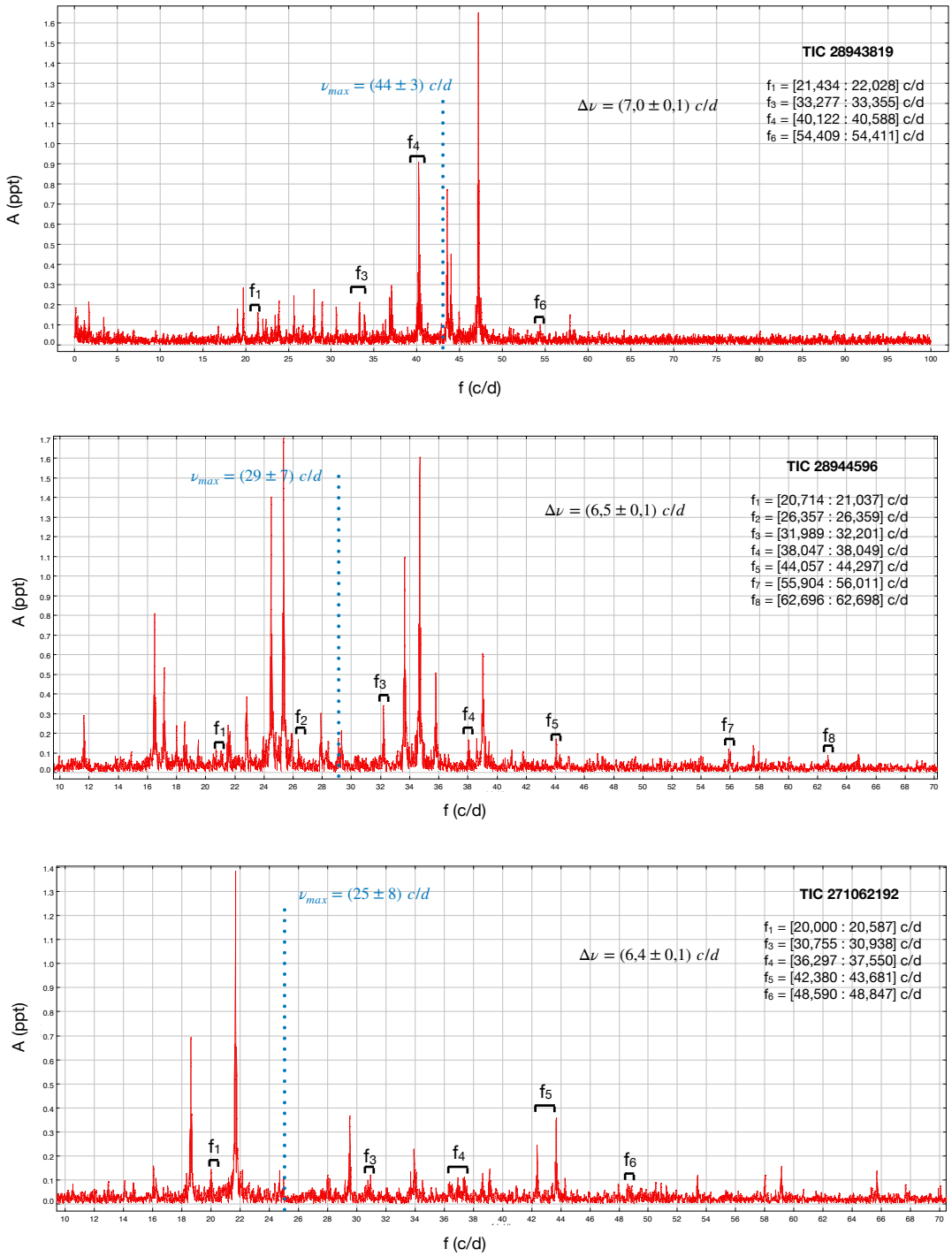

Fig. 10: Identified radial overtones in the frequency spectrum of three of the δ Sct stars candidates in the field of Trumpler 10

A. The estimated large separations of our δ Sct stars sample

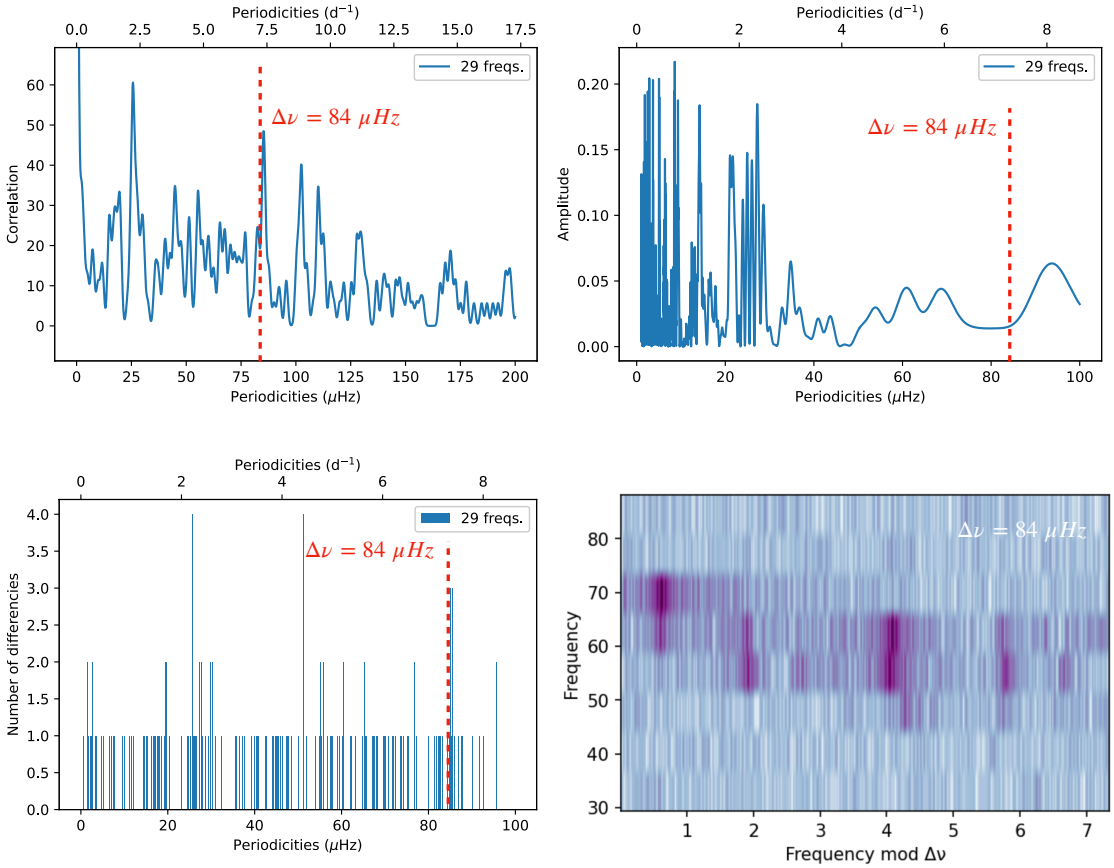

Fig. A.1: The same as Fig. 5 for TIC 30307085

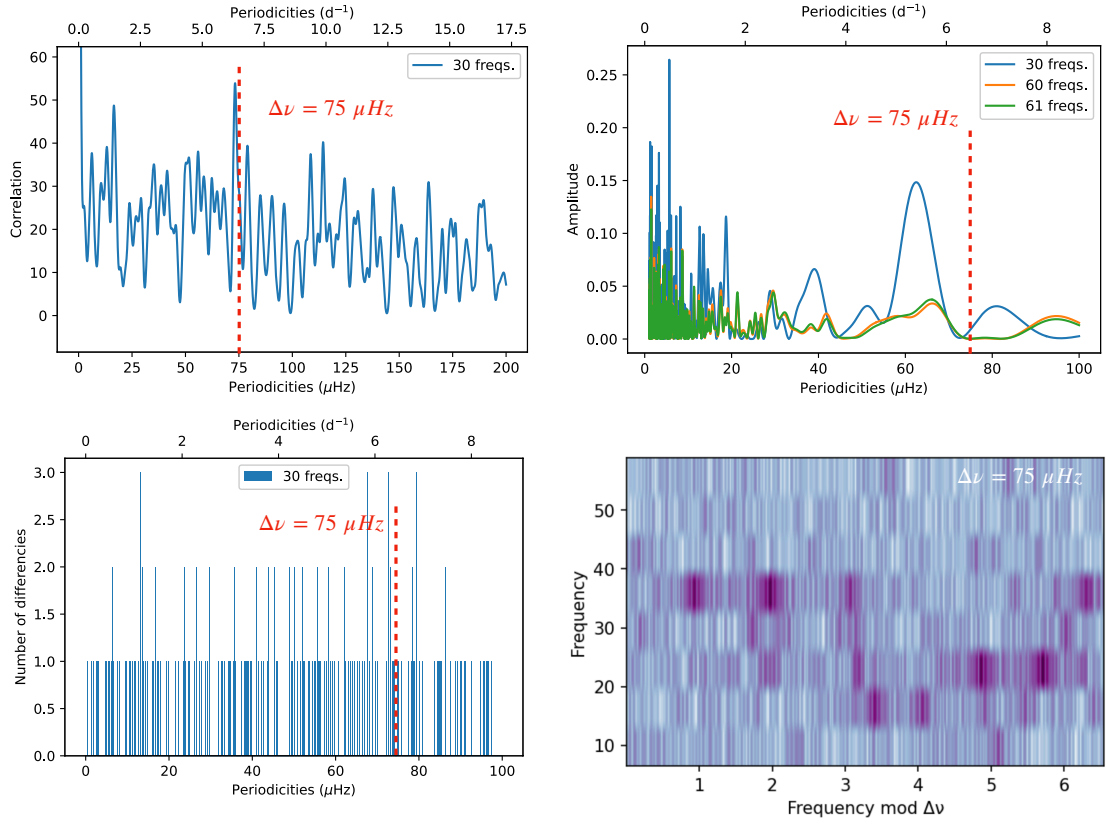

Fig. A.2: The same as Fig. 5 for TIC 28944596

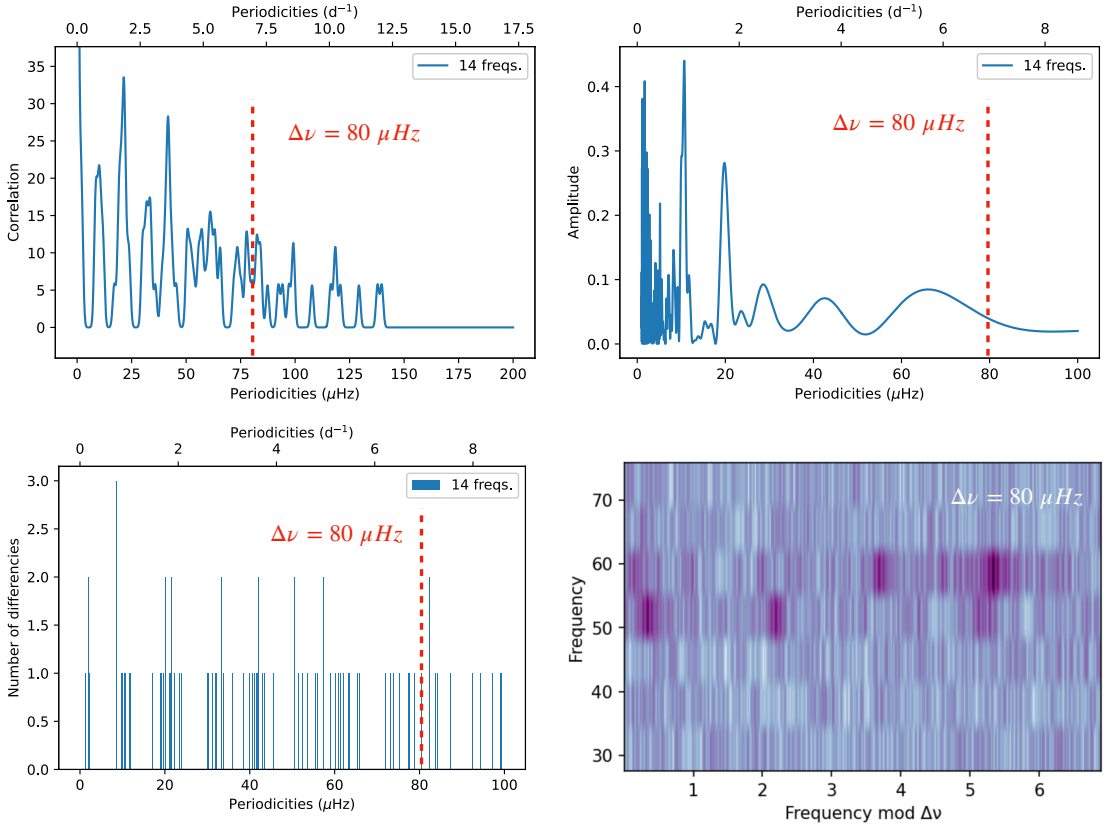

Fig. A.3: The same as Fig. 5 for TIC 271061334

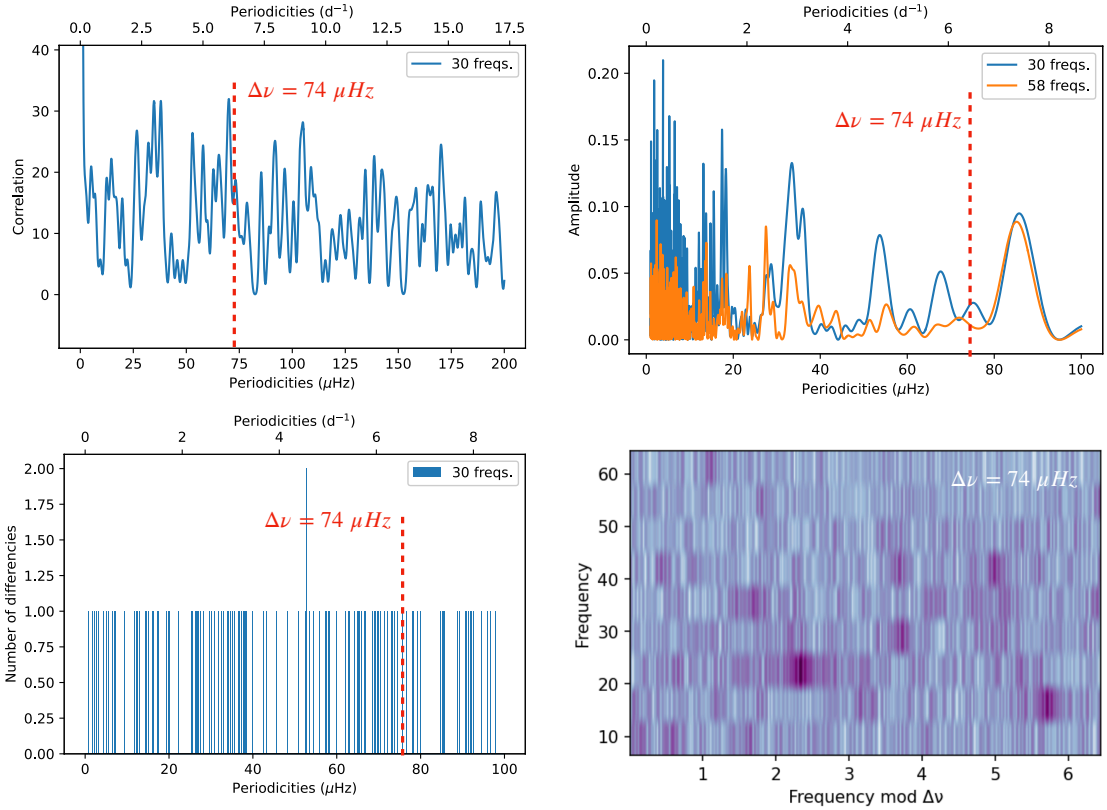

Fig. A.4: The same as Fig. 5 for TIC 271062192

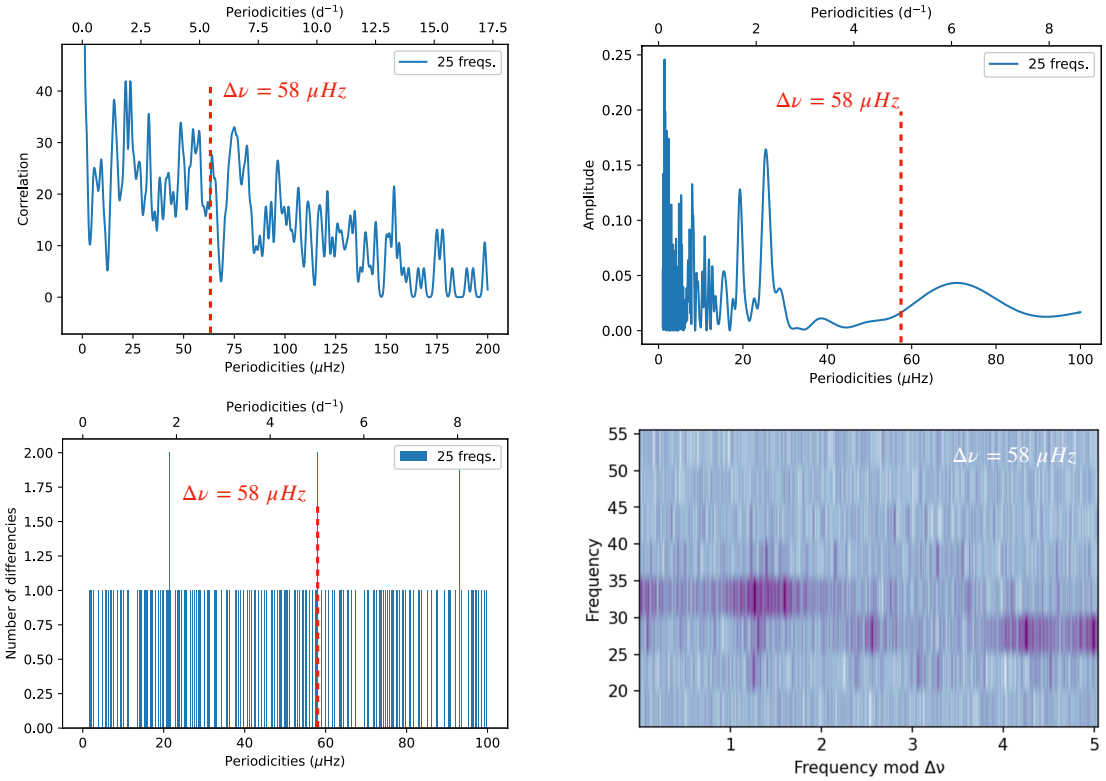

Fig. A.5: The same as Fig. 5 for TIC 175194881

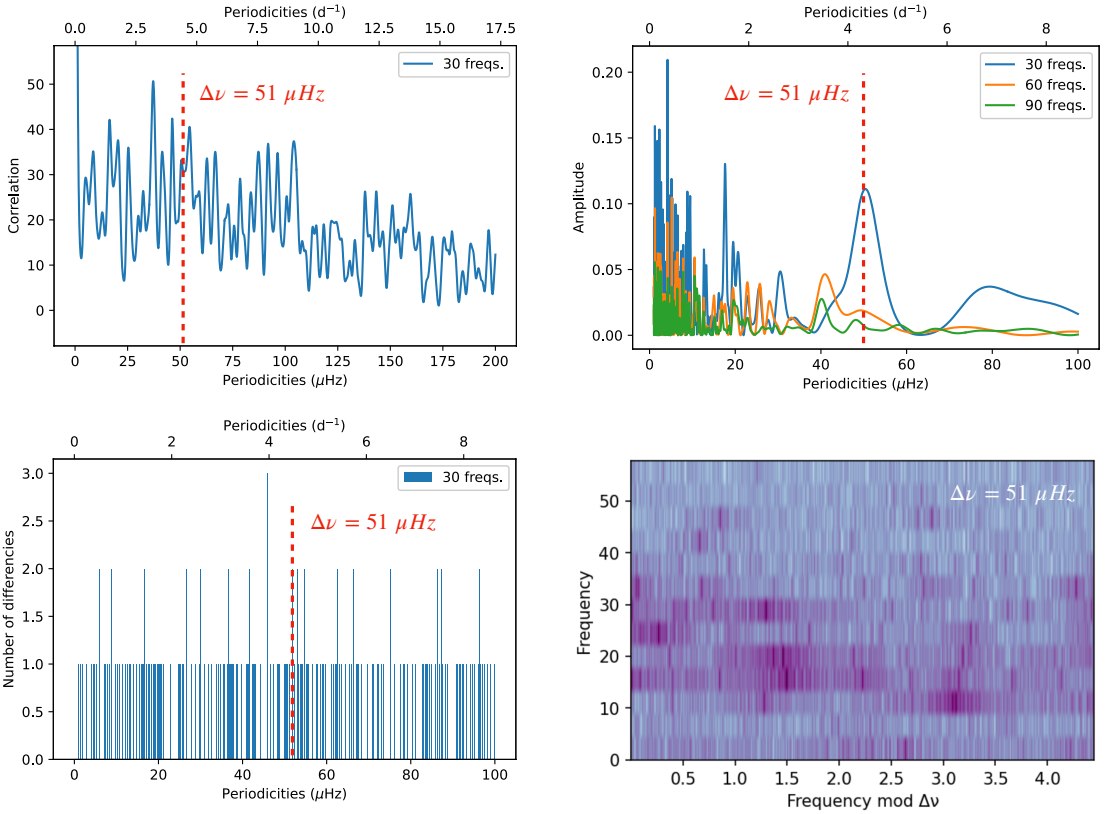

Fig. A.6: The same as Fig. 5 for TIC 175264376

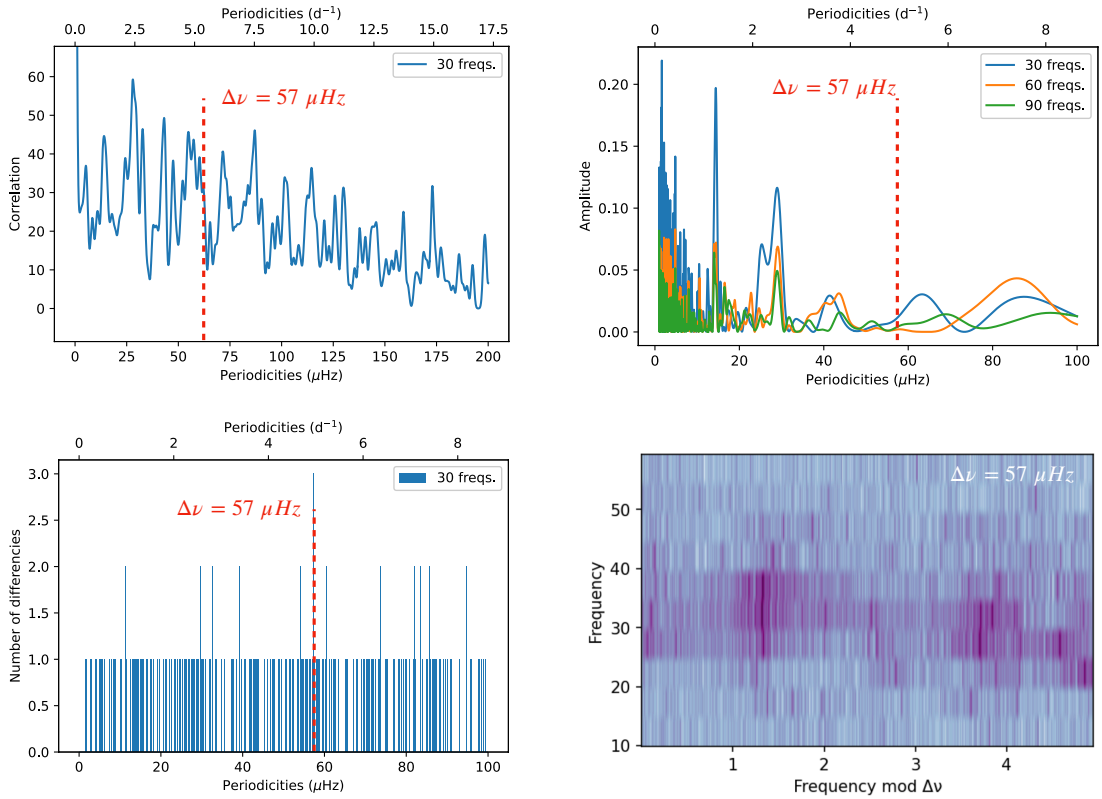

Fig. A.7: The same as Fig. 5 for TIC 175265807

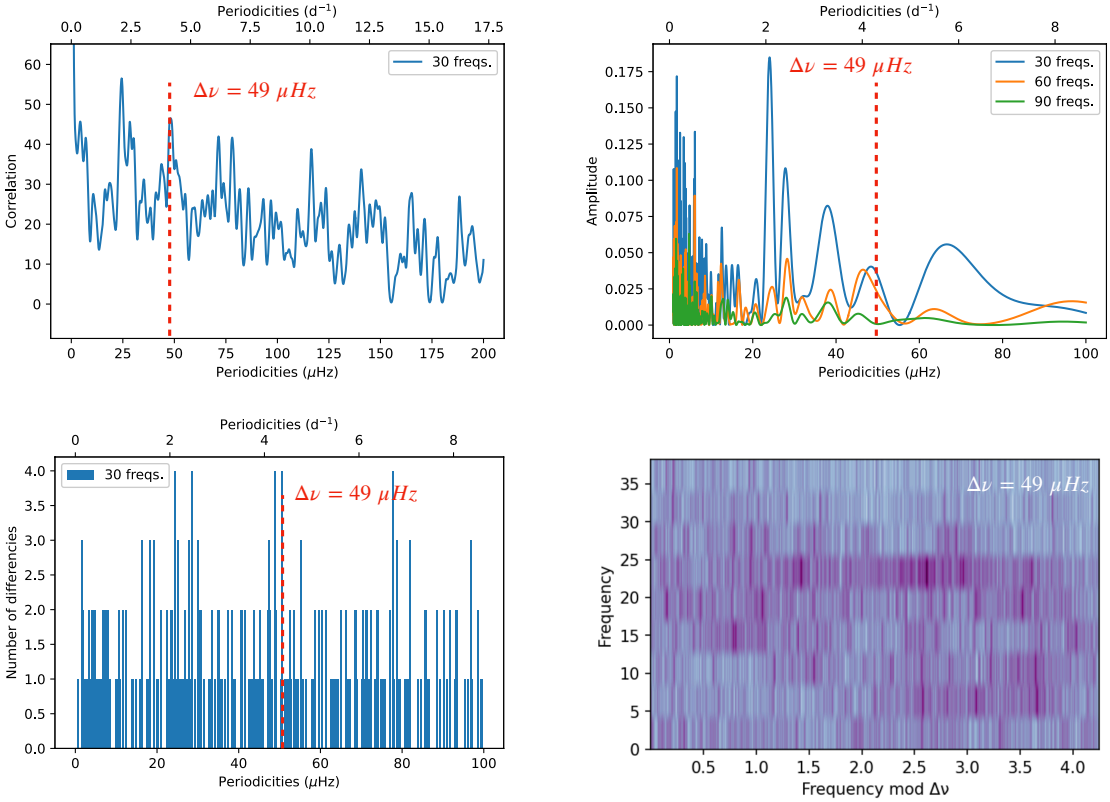

Fig. A.8: The same as Fig. 5 for TIC 175291778

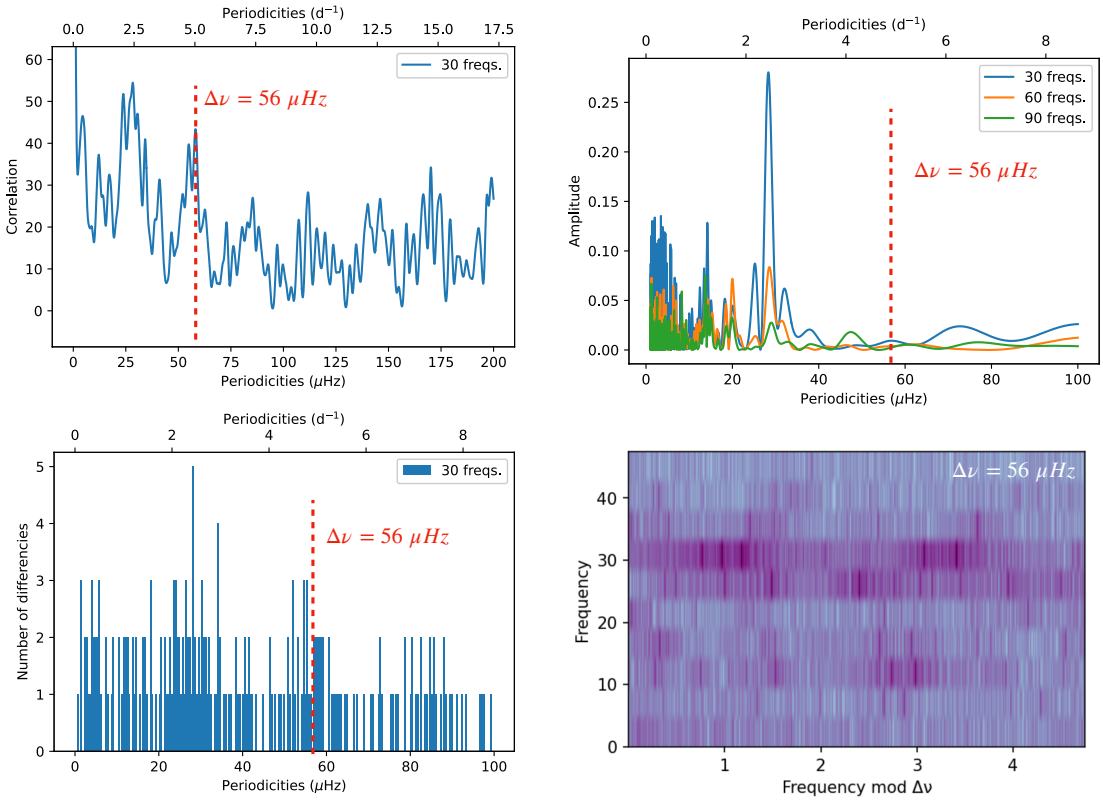

Fig. A.9: The same as Fig. 5 for TIC 184914505

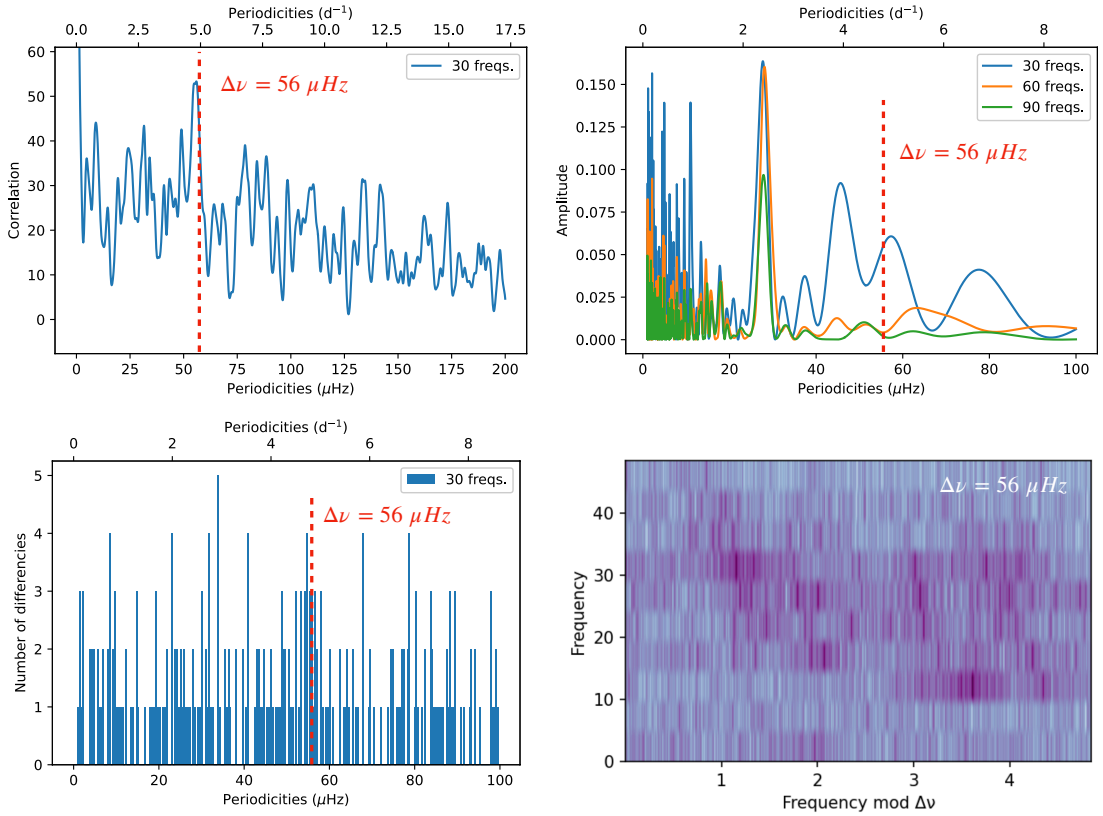

Fig. A.10: The same as Fig. 5 for TIC 184917633